Arabian Journal of Chemistry (2021) **14**, 102960

King Saud University

Arabian Journal of Chemistry

www.ksu.edu.sa
www.sciencedirect.com

REVIEW ARTICLE

Study of adsorption property and mechanism of lead(II) and cadmium(II) onto sulfhydryl modified attapulgite

Cheng Fu [a], Xiaping Zhu [a,*], Xun Dong [a], Ping Zhao [b], Zepeng Wang [b]

[a] *College of Materials and Chemistry and Chemical Engineering, Chengdu University of Technology, Chengdu 610059, China*
[b] *Geological Party 105, Guizhou Provincial Bureau of Geology and Mineral Exploration and Development, Guiyang 550018, China*

Received 27 November 2019; accepted 19 January 2020
Available online 21 December 2020

KEYWORDS

Sulfhydryl modified attapulgite;
Lead and cadmium;
Adsorption properties;
Adsorption mechanism

Abstract Study of the adsorption property and mechanism about the environmental functional material can provide theoretical guidance for its actual application. The sulfhydryl attapulgite (SH-ATP) was prepared by solution blending method. The saturated adsorption capacity to Pb^{2+} and Cd^{2+} in the experiment were 65.57 and 22.71 mg/g, which increased by 57.74% and 31.96% comparing with the attapulgite (ATP), respectively. The adsorption kinetics experiments illustrated that the adsorption of Pb^{2+} and Cd^{2+} onto SH-ATP accorded with multiple kinetic models. Among them, the pseudo second-order model had the best correlation, the correlation coefficients were all above 0.998. The adsorption thermodynamics experiments testified that the adsorption of Pb^{2+} and Cd^{2+} onto SH-ATP conformed to the Langmuir, Tempkin and Dubinin-Radushkevich models, those models indicated that the adsorption processes belonged to the monolayer adsorption, the adsorbent surface was homogeneous, and the micropore distribution of the adsorbent was also relatively uniform. Various thermodynamic parameters ($\Delta H > 0$, $\Delta S > 0$, $\Delta G < 0$) under 25-45℃ indicated that the adsorption processes of Pb^{2+} and Cd^{2+} onto SH-ATP were endothermic and spontaneous.

Contents

* Corresponding author at: Erxianqiao Dongsan Road 1#, Chengdu, China.
E-mail address: zhuxiaping@cdut.edu.cn (X. Zhu).
Peer review under responsibility of King Saud University.

Production and hosting by Elsevier

https://doi.org/10.1016/j.arabjc.2020.102960

1. Introduction

In recent decades, the development of industry and agriculture has caused heavy metals pollution such as lead and cadmium in soil and water, which poses a serious threat to the human living environment. The lead and cadmium are toxic metals, which are extremely harmful. Once lead and cadmium are introduced into the environment, which can hardly be degraded by chemical reactions or microbial activities (Zeng et al., 2017). The large-scale pollution accidents were caused by lead and cadmium, which occurred frequently in the history of human health. Japanese Itai-Itai Disease event was caused by cadmium poison. In Australia and New Zealand, cadmium accumulated in the viscera of grazing animals, making them inedible for human. Moreover, the lead-contaminated water event in Flint Michigan made a large number of local residents suffer from diseases such as nerves, hematopoiesis and kidneys.

At present, the remediation methods of lead and cadmium pollution soil and water mainly include electrochemical repair, adsorption, chemical precipitation and phytoremediation. Among them, the adsorption method has received great attention due to its high efficiency and low cost (Mondal, 2009). Now researchers have developed various adsorbents. Such as the maximal adsorption capacities for lead and cadmium by lipopeptides modified Na-montmorillonite were 20.3 and 19.5 mg/g, respectively (Zhu et al., 2013b). For another example, peat as a low-cost adsorbent removed Ni^{2+} and Pb^{2+} from aqueous solutions, and the adsorption capacities for Ni^{2+} and Pb^{2+} were 61.27 and 82.31 mg/g (Bartczak et al., 2018). Also, Bhattacharyya explored the various modified clays, in which the maximal adsorption capacities of lead and cadmium onto acidified modified montmorillonite reached 34.0 and 21.4 mg/g (Bhattacharyya and Sen Gupta, 2008). Other adsorbents such as Graphene Oxides, coconut, coir and biochar (Aliabadi et al., 2014; Yang et al., 2015; Revathi et al., 2016; Karunanayake et al., 2018) were also often used to restore lead and cadmium pollution in soil and water.

Now more and more attention focuses on removal of heavy metals from soil and wastewater by clay (Zhang et al., 2010; Arancibia-Miranda et al., 2016; Ma et al., 2017). It is because clay mineral has large surface areas, stable chemical, mechanical properties and a wide range of sources (Wang et al., 2007). Palygorskite is a clay mineral, also known as attapulgite (ATP), it is a kind of 2:1 layered hydrated magnesium aluminum silicate minerals with two bands of silica tetrahedra linked by magnesium ions in octahedral coordination (Yariv et al., 2011; Zhu et al., 2016). The ATP mainly contains Mg^{2+} and other cations such as Fe^{3+} and Al^{3+} (Gionis et al., 2007), which is fibrous, porous, charge in the lattice, abundant in reserve and environmentally friendly, and it has adsorption properties, cation exchangeability (Zhang et al., 2015). However, natural ATP often contains many impurities, so the adsorption capacity to heavy metals is low, the adsorptive force is weak, and natural ATP has non-specific adsorptivity. In order to improve its absorptivity, it is often modified, such as acid modification to remove impurities and increase specific surface area (Barrios et al., 1995), thermal modification to remove water molecules in the pore canal (Wang et al., 2012), and organic modification to enhance chemisorption capacity, etc. (Sarkar et al., 2011; Liang et al., 2013).

At present, there are few reports on sulfhydryl functionalized ATP. In addition to, the study on the adsorption mechanism to heavy metals is also very scarce. Krikorian used azeotropic distillation to treat attapulgite with 2-mercaptoethanol, the obtained material could remove > 90% of 1.57 mmol/L of Pb^{2+} and Cd^{2+} (Krikorian and Martin, 2005). Liang successfully prepared sulfhydryl functionalized ATP by high-speed shearing method based on the rheological properties, and increased the adsorption capacities of Pb^{2+}, Cd^{2+} and Cu^{2+} to 66.30, 30.35 and 25.42 mg/g (Liang et al., 2013). These modifications are complicated and expensive.

We used the solution blending method to modify the ATP (without any purification) with 3-mercaptopropyltrimethoxysi lane, adding polyethylene glycol to improve the solid-liquid interface properties and enhance the dispersion effect of the ATP. The sulfhydryl groups grafted on the surface and interlayer of ATP markedly enhanced the adsorption to lead and cadmium. And we deeply explored the adsorption capacity, adsorption kinetics and adsorption thermodynamics, and clarified adsorption mechanism of modified material (SH-ATP) to lead and cadmium. All adsorption experiments were carried out on the condition of adding a certain amount of KNO_3 which simulate the interference of other ions in the actual application. The study provides theoretical guidance for the application of SH-ATP in the remediation of lead and cadmium contaminated soil or water.

Table 1 Main chemical composition of attapulgite.

Composition	Na_2O	MgO	Al_2O_3	SiO_2	K_2O	CaO	Fe_2O_3	Total
Content (%)	0.70	7.68	8.50	40.44	1.47	15.96	5.02	79.77

2. Experimental

2.1. Instruments and reagents

Tensor-27 Fourier transform infrared spectrometer (Bruker Daltonik GmbH, Germany), DX- 2700 X-ray diffractometer (Dandong Fangyuan Instrument Company, China), STA409PCLuxx Simultaneous thermal gravimetric analyzer (NETZSCH Machinery and Instruments Co., Ltd., Germany), AA1700 atomic absorption spectrometer (Zhejiang Fuli Analytical Instruments Inc, China).

The attapulgite was from Baiyin City, Gansu, China. The specific compositions are showed in Table 1. 3-Mercaptopropyltrimethoxysilane (SH) (>98%), $Pb(NO_3)_2$, $Cd(NO_3)_2{\cdot}4H_2O$, KNO_3 and KOH were provided by Chengdu Chron Chemicals Co,.Ltd (Chengdu, China), and were of analytical grade.

2.2. Preparation of SH-ATP

SH-ATP was prepared with SH as modifier. 1.000 g of dry ATP was dispersed in 50.00 mL of ethanol solution with 5% 3-mercaptopropyltrimethoxysilane, and a small amount of polyethylene glycol was added, then the mixed solution was stirred for 7 h at room temperature. The precipitate was filtered, washed with distilled water, dried in vacuum at 60 °C, and then ground into powder.

2.3. Adsorption experiments

The solutions of Pb^{2+} and Cd^{2+} were prepared by dissolving the corresponding amount of metal salt in deionized water. The solutions and 0.250 g of SH-ATP were shaken on a rotary shaker. Adding KNO_3 as an adsorption medium, the concentration of KNO_3 was kept to 0.1 mol/L. According to the experimental results--the effect of pH on the adsorption of lead and cadmium by SH-ATP, it was finally determined that the pH of solutions were adjusted to 6.0 (Pb^{2+}) and 6.5 (Cd^{2+}) with 0.1 mol/L NaOH and 0.1 mol/L HCl. The mixed solutions were vibrated for 2 h at room temperature, and were centrifuged at 3500 r/min for 10 min, then the supernatant was kept for analyzing Pb^{2+} and Cd^{2+} with an atomic adsorption spectrometer. The adsorption rate η (%) and the adsorption capacity Q_a (mg/g) were calculated according to formula (2-1) and (2-2).

$$\eta = \frac{c_0 - c_e}{c_0} \times 100\% \quad (2\text{-}1)$$

$$Q_a = \frac{v(c_0 - c_e)}{1000m} \quad (2\text{-}2)$$

where v is the volume of the adsorption solution (mL), m is the amount of SH-ATP (g), c_0 and c_e are the concentration of Pb^{2+} or Cd^{2+} in the solution before and after adsorption (mg/L).

2.4. Adsorption kinetics experiment

Adsorption kinetics is one of the important characteristics that defines the efficiency of an adsorbent, which can describe the adsorption rate of an adsorbent and explore the adsorption mechanism. The adsorption rate of the adsorbent is evidently controlled by the diffusion process and the residence time of the adsorbate adsorbed at the solid solution interface. Adsorption kinetics can be controlled by several independent processes acting in parallels or in series. These processes are externally mass transfer, bulk diffusion, intra-particle diffusion, and chemisorption. In order to determine the solute uptake rate and explain the transport of Pb^{2+} and Cd^{2+} to the surfaces of SH-ATP, different kinetic models were employed (see Table 2).

Referring to the content of 2.3 above, the Pb^{2+} concentrations were 400, 600 and 800 mg/L, respectively, the adsorption time were 2, 5, 10, 20, 30, 45, 60, 120, 180, 240, 360, 540, 720, 1080, 1440, 1800, 2160 min. The Cd^{2+} concentrations were 100, 200 and 400 mg/L, respectively, the adsorption time were 2, 5, 10, 20, 30, 45, 60, 120, 180, 240, 360, 540, 720, 1080, 1440 min. Adsorption datum were fitted with pseudo first-order model, pseudo second-order model, Elovich model, dual constant model and Webber–Morris model (Ijagbemi et al., 2010; Javadian et al., 2015).

2.5. Adsorption thermodynamics experiment

Referring to the content of 2.3 above, the experiments were carried out at temperature of 288.15, 298.15, 308.15 and 318.15 K, respectively. The Pb^{2+} concentrations were 10, 20, 50, 100, 200, 400, 600, 800, 1200, 1600, and 2000 mg/L, respectively. The Cd^{2+} concentrations were 20, 50, 100, 200, 300, 400, 500, 600, 650, 700, 750 and 800 mg/L, respectively.

Acquired equilibrium data were fitted with different adsorption isotherm models (see Table 3), in order to have

Table 2 The kinetics models and expression.

Adsorption kinetics	Expression
Pseudo first-order model	$\ln(q_e - q_t) = \ln q_e - k_1 t$
Pseudo second-order model	$\frac{t}{q_t} = \frac{1}{k_2 q_e^2} + \frac{t}{q_e}$
Elovich model	$q_t = \frac{1}{\tau}\ln(\alpha\tau) + \frac{1}{\tau}\ln t$
Dual constant model	$\ln q_t = a + b\ln t$
Webber–Morris model	$q_t = k_{id} t^{0.5}$

Where q_e is adsorption capacity at equilibrium (mg/g), q_t is adsorption capacity at any time t (mg/g), t is time (min), k_1 is rate constant of first-order adsorption (min^{-1}), k_2 is rate constant of second-order adsorption (g/mg·min), α is related to rate of chemisorption, τ is related to surface coverage, b is constant related to the extent of adsorption (L/mg) and k_{id} is intraparticle diffusion rate constants.

Table 3 The thermodynamics models and expression.

Adsorption isotherm models	Expression
Langmuir model	$\frac{c_e}{q_e}=\frac{c_e}{Q_m}+\frac{1}{K_L Q_m}, R_L=\frac{1}{1+K_L c_0}$
Freundlich model	$\ln q_e=\ln K_f+\frac{1}{n}\ln c_e$
D-R model	$\ln q_e=\ln Q_{DR}-\gamma\varepsilon^2, \varepsilon=RT\ln(1+\frac{1}{c_e}), E=(-2\gamma)^{-0.5}$
Tempkin model	$q_e=B_T lnA_T+B_T lnc_e, B_T=RT/b_T$
Florry–Huggins model	$\log\frac{\theta}{c_0}=\log K_{FH}+\lambda\log(1-\theta), \theta=1-c_e/c_0$

Where c_e is equilibrium concentration (mg/L), K_L is intensity of adsorption (L/mg), Q_m is maximum adsorption at monolayer coverage (mg/g), R_L is dimensionless separation factor, c_0 is initial concentration (mg/L), K_f is freundlich adsorption constant, 1/n is adsorption index, Q_{DR} is D–R adsorption capacity (mg/g), ε is polanyi potential, γ is D–R adsorption energy constant (mol^2/kJ^2), E is sorption energy (kJ/mol), B_T is tempkin isotherm energy constant (dimensionless), A_T is tempkin adsorption potential (L/mg), b_T is tempkin heat of sorption (kJ/mol), θ is rate of surface coverage, λ is the amount of adsorbate occupying the active sites of the adsorbent and K_{FH} is equilibrium constant.

insight into the sorption mechanisms, surface properties and affinities of SH-AT for Pb^{2+} and Cd^{2+} adsorption. The adsorption datum were fitted by the Langmuir model, the Freundlich model, the D-R (Dubinin-Radushkevich) model, the Tempkin model, and the Florry-Huggins model (Freundlich, 1906; Langmuir, 1918; Eren, 2009).

3. Results and discussion

3.1. The saturated adsorption of Pb^{2+} and Cd^{2+} onto ATP and SH-ATP

The saturated adsorption curves of Pb^{2+} and Cd^{2+} onto ATP and SH-ATP were exhibited in Fig. 1. With the increase of Pb^{2+} and Cd^{2+} concentrations, the adsorption capacities of ATP and SH-ATP were increasing, and the adsorption capacity of SH-ATP was more than that of ATP. ATP and SH-ATP reached the maximal adsorption capacity at Pb^{2+} concentration of 800 mg/L and Cd^{2+} concentration of 400 mg/L. The saturated adsorption capacities of ATP and SH-ATP to Pb^{2+} and Cd^{2+} (25 °C) were 41.57 and 65.57 mg/g, 17.21 and 22.71 mg/g, respectively. Compared with the ATP, the saturated adsorption capacities of Pb^{2+} and Cd^{2+} had a significant enhancement, and increased by 57.74% and 31.96%, respectively.

Table 4 showed the results of adsorption of Pb^{2+} and Cd^{2+} on sulfhydryl modified clay minerals reported in some literature.

Table 4 Compared with maximum adsorption capacity of different sulfhydryl functionalized clay.

Adsorbents samples	Sorption capacity (mg/g)	References
Thiol-montmorillonite	Pb 72.52 Cd 26.67	Mercier and Detellier, 1995
2-mercaptoethanol montmorillonite	Pb 4.31 Cd 4.54	Krikorian and Martin, 2005
Mercaptoethanol-modified silica	Pb 10.42 Cd 4.75	Kosak et al., 2015
MSEF-NT	Pb 116.03 Cd 34.85	Liang et al., 2011
MSEF-GF	Pb 64.23 Cd 23.60	Liang et al., 2011
XYPAL-SH	Pb 66.30 Cd 30.35	Liang et al., 2013
MPS-SEP	Pb 10.77	Celis et al., 2000
$MEAMONT_{50}$	Pb 48.90	Celis et al., 2000
MMT-SH	Cd 22.23	Zhu et al., 2013a
TFB	Pb 67.27	Xiong et al., 2012
SH-ATP	Pb 65.57 Cd 22.71	This work

Where MSEF-NT: 3-mercaptopropyltrimethoxysilane modified sepiolite of nanotexturization, MSEF-GF: 3-mercaptopropyltrimethoxysilane modified sepiolite, XYPAL-SH: 3-mercaptopropyltrimethoxysilane modified palygorskite, MPS-SEP: 3-mercaptopropyltrimethoxysilane modified sepiolite, MEAMONT 50: 2-mercaptoethylammonium modified montmorillonite, MMT-SH: mercaptan modified montmorillonite, TFB: 3-mercaptopropyltrimethoxysilane modified bentonite.

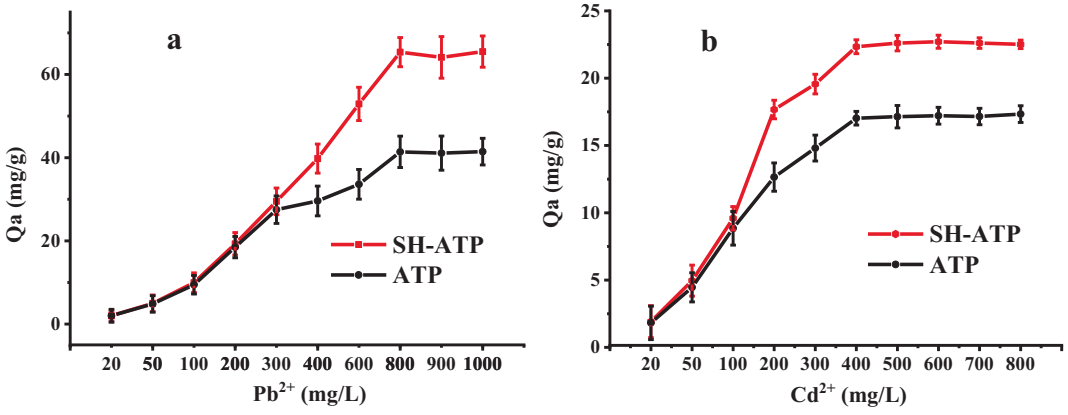

Fig. 1 The adsorption of Pb^{2+} (a) and Cd^{2+} (b) onto SH-ATP and ATP.

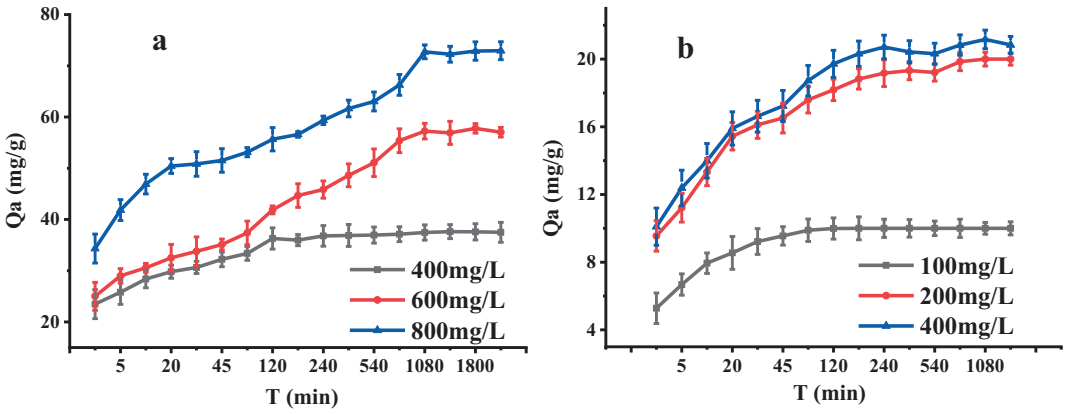

Fig. 2 Adsorption kinetics of Pb^{2+} (a) and Cd^{2+} (b) onto SH-ATP.

tures. Except in that of Liang (Liang et al. 2011), the adsorption capacities of SH-ATP for Pb^{2+} and Cd^{2+} were comparable to the counterpart reported in other literatures, or were better than those. However, in other researches, ATP often require purification, or the modification process was complex and time consuming, and the modification cost was high, most of the literatures did not consider actual interference in studying the adsorption capacities of materials. The ATP used in this study had not been purified, the modification process was simple, fast, and inexpensive. Moreover the measure of adding a certain amount of KNO_3 in the adsorption experiment fully considered the possible interference in actual application, so that the obtained results had the practical application value.

3.2. Fitting results of adsorption kinetics models

The experiments about adsorption kinetics of Pb^{2+} and Cd^{2+} onto SH-ATP were carried out according to the experimental method described in 2.4. The results were shown in Fig. 2. The adsorption of Pb^{2+} and Cd^{2+} onto SH-ATP could be divided into different stages. At first, the adsorption rate increased, and eventually tended to balance with the increase of time. When the concentrations of Pb^{2+} and Cd^{2+} were larger, the absorption equilibrium time was longer, and there were more and more stages of absorption. When the concentrations of Pb^{2+} were 400, 600 and 800 mg/L, the experimental equilibrium adsorption capacities of SH-ATP to Pb^{2+} were 37.2, 57.1 and 72.3 mg/g, respectively. When the concentrations of Cd^{2+} were 100, 200 and 400 mg/L, the experimental equilibrium adsorption capacities were 10.0, 19.2 and 21.5 mg/g, respectively.

Table 5 showed that the relevant parameters were obtained from the experimental data which were fitted into kinetic model. Based on the fitting correlation coefficient, the Pseudo second-order model described the adsorption of Pb^{2+} and Cd^{2+} onto SH-ATP, which was better than Dual constant model, Elovich model and Pseudo first-order model, and the fitting result of Webber-Morris model was worst.

When Pb^{2+} concentration of 400, 600 and 800 mg/L were adsorbed by SH-ATP, the correlation coefficients of the Pseudo second-order model were > 0.998, and the adsorption rate constant decreased with increasing of Pb^{2+} concentration. The calculated adsorption amounts were 37.59, 58.14 and 73.53 mg/L, which were in good agreement with the experimental values (37.2, 57.1 and 72.3 mg/L). When Cd^{2+} concentration of 100, 200 and 400 mg/L were adsorbed by SH-ATP, the correlation coefficients of the Pseudo second-order model were greater than 0.999. The adsorption rate constant decreased with increasing of Cd^{2+} concentration, compared with Pb^{2+}, the rate constant was decreased more evidently. The calculated adsorption amounts were 10.02, 20.08 and 21.01 mg/L, which were well accord with the experimental values (10.0, 19.2 and 21.5 mg/L). The fitting results of the Pseudo second-order model showed that the adsorption of Pb^{2+} and Cd^{2+} might have taken place via surface exchange reactions until the surface functional sites were completely occupied, subsequently Pb^{2+} and Cd^{2+} diffuse into the SH-ATP layers for further interactions such as ion-exchange and complexation. Similar result was reported by Fan (Fan et al., 2008; Zheng et al., 2018).

3.3. Fitting results of adsorption thermodynamics model

The adsorption results of Pb^{2+} and Cd^{2+} onto SH-ATP at different temperatures were shown in Fig. 3. With the increase of Pb^{2+} and Cd^{2+} concentrations, the adsorption capacities gradually increased, and finally reached saturation, and the saturated adsorption capacities increased with increasing temperature. When the concentrations of Pb^{2+} and Cd^{2+} were less than 400 and 100 mg/L, respectively, the adsorption capacities were not much distinct at different temperatures, but with the increase of concentration, the effect of temperature was more and more obvious. In general, physical adsorption was an exothermic reaction, while chemisorption was an endothermic reaction. When the concentrations of Pb^{2+} and Cd^{2+} were low, primary adsorption forces of SH-ATP were physical adsorption such as electrostatic attraction and ion exchange. When the concentrations of Pb^{2+} and Cd^{2+} were high, the hydroxyl groups and the grafted sulfhydryl groups of SH-ATP could form complexation with Pb^{2+} and Cd^{2+}. At temperature of 288.15, 298.15, 308.15 and 318.15 K, the saturated adsorption capacities of SH-ATP onto Pb^{2+} and Cd^{2+} in the experiment were 63.40, 65.62, 69.53, 78.45 mg/L and 18.71, 19.83, 21.25, 22.89 mg/L, respectively.

The Tempkin model assumed a linear decrease in heat of adsorption with surface coverage. The D–R model can be used to estimate the characteristic porosity of adsorbents and their

Table 5 Adsorption kinetics parameters.

Metals ion	Models	Parameters	400 mg/L	600 mg/L	800 mg/L
		q_e Exp.(mg/g)	37.2	57.1	72.3
Pb^{2+}	Pseudo first-order model	k_1	0.0122	0.0025	0.0026
		q_e Cal.(mg/g)	37.46	57.24	72.70
		R^2	0.9169	0.9560	0.9531
	Pseudo second-order model	k_2(g/mg min)	0.0266	0.0172	0.0136
		q_e Cal.(mg/g)	37.59	58.14	73.53
		R^2	1	0.9989	0.9984
	Elovich model	α (g/mg min)	$2.42E^5$	$2.09E^2$	$2.39E^3$
		τ (mg/g)	0.49	0.20	0.19
		R^2	0.9147	0.9509	0.9718
	Dual constant model	α (mg/g min)	3.1942	3.1470	3.5672
		b	0.0649	0.1222	0.0967
		R^2	0.9845	0.9705	0.9667
	Webber-Morris model	α (mg/g $min^{1/2}$)	29.5766	30.983	45.071
		b	0.2372	0.7093	0.7210
		R^2	0.5916	0.8913	0.8725
Metals ion	Models	Parameters	100 mg/L	200 mg/L	400 mg/L
		q_e Exp.(mg/g)	10.0	19.2	21.5
Cd^{2+}	Pseudo first-order model	k_1	0.0517	0.2004	0.0067
		q_e Cal.(mg/g)	10	19.95	20.66
		R^2	0.9865	0.8684	0.7157
	Pseudo second-order model	k_2(g/mg min)	$6.22E^{-2}$	$5.66E^{-3}$	$7.13E^{-3}$
		q_e Cal.(mg/g)	10.02	20.08	21.01
		R^2	1	0.9998	0.9998
	Elovich model	α (g/mg min)	$1.58E^4$	$8.40E^2$	$9.35E^2$
		τ (mg/g)	1.60	0.64	0.60
		R^2	0.752	0.9233	0.9137
	Dual constant model	α (mg/g min)	1.8447	2.3398	2.4010
		b	0.0787	0.1045	0.1037
		R^2	0.7094	0.8743	0.8743
	Webber-Morris model	α (mg/g $min^{1/2}$)	8.0513	13.829	14.697
		b	0.0774	0.2223	0.2315
		R^2	0.3847	0.6134	0.5932

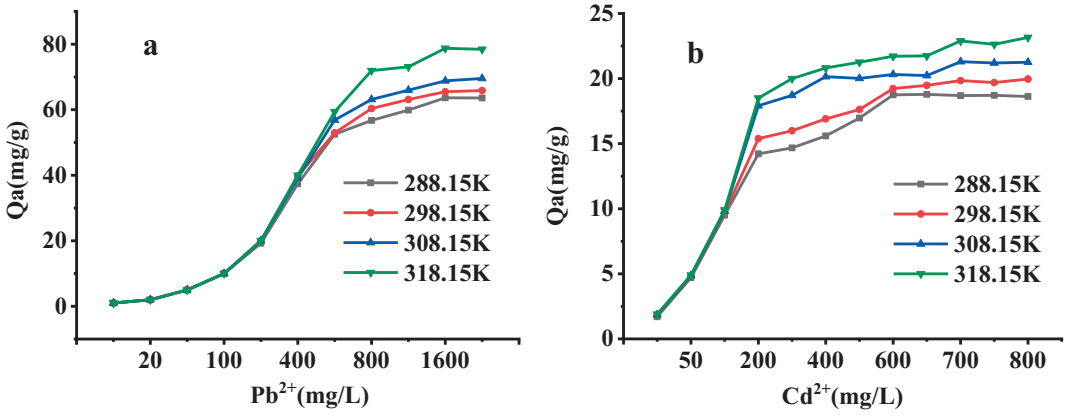

Fig. 3 Adsorption isotherm of Pb^{2+}(a) or Cd^{2+}(b) onto SH-ATP.

apparent energy of adsorption. Table 6 showed that the Temp-kin and the D-R models agreed well with the experimental data, as the temperature increased, the adsorption capacity also increased (consistent with the experimental results), indicated that there was an interaction between SH-ATP and Pb^{2+}(or Cd^{2+}), and the micropore distribution of the SH-ATP was relatively uniform.

When the Freundlich model was used to fit the Pb^{2+} and Cd^{2+}adsorptive datum, the correlation coefficient (R^2) for Pb^{2+} adsorption were in 0.7612–0.8555, and for the Cd^{2+},

Table 6 Adsorption thermodynamic parameters.

Metals ion	Models	Parameters	288.15 K	298.15 K	308.15 K	318.15 K
Pb^{2+}	Langmuir	Q_m (mg/g)	63.29	65.79	68.03	78.13
		K_L (L/mg)	0.0667	0.3071	0.0985	0.1860
		R^2	0.9973	0.9999	0.9967	0.9994
	Freundlich	K_f	8.279	16.333	19.397	32.233
		$1/n_f$	0.3279	0.2455	0.1985	0.1496
		R^2	0.8555	0.7791	0.7612	0.8056
	Tempkin	A_T	7.443	33.780	130.73	1300.3
		B_T	7.0942	6.6963	5.8297	5.7834
		R^2	0.9582	0.9344	0.9232	0.9440
	D-R	Q_{DR} (mg/g)	46.115	60.29	58.82	71.42
		E (kJ/mol)	1.581	2.236	5.000	5.000
		R^2	0.9070	0.9767	0.9284	0.9641
	Florry-Huggins	λ	−0.8756	−0.6022	−0.4673	−0.3571
		K_{HF}	$2.15E^{-4}$	$2.40E^{-4}$	$3.11\ E^{-4}$	$2.83\ E^{-4}$
		R^2	0.8467	0.8425	0.7753	0.8872
Metals ion	Models	Parameters	288.15 K	298.15 K	308.15 K	318.15 K
Cd^{2+}	Langmuir	Q_m (mg/g)	19.38	20.24	21.32	22.94
		K_L (L/mg)	0.0378	0.0480	0.0968	0.0986
		R^2	0.9946	0.9957	0.9987	0.998
	Freundlich	K_f	7.568	8.575	10.257	11.131
		$1/n_f$	0.1426	0.1318	0.1191	0.1173
		R^2	0.9672	0.9733	0.8718	0.9026
	Tempkin	A_T	5.155	51.865	270.837	418.287
		B_T	2.3408	1.8967	1.7938	1.8525
		R^2	0.9486	0.9624	0.9114	0.941
	D-R	Q_{DR} (mg/g)	17.070	18.198	20.223	21.383
		E (kJ/mol)	0.408	0.707	0.791	1.581
		R^2	0.9396	0.9571	0.9779	0.9319
	Florry-Huggins	λ	−1.5025	−1.2765	−1.1287	−0.9523
		K_{HF}	$3.48E^{-4}$	$3.80\ E^{-4}$	$3.92\ E^{-4}$	$4.40\ E^{-4}$
		R^2	0.7908	0.8011	0.8095	0.7986

the range were 0.8718–0.9733. The $1/n_F$ values yielded from Freundlich model were less than 1, and as temperature rose, $1/n_F$ were getting smaller and smaller (It was consistent with the conclusion of the thermodynamic experiment, the adsorption was the easier, as the temperature increased), indicating that Pb^{2+} and Cd^{2+} were favourably adsorbed by SH-ATP. This type of behavior had also been reported by Tahir and Rauf (2003).

The Florry-Huggins isotherm was not fitted into the adsorption of Pb^{2+} and Cd^{2+} onto SH-ATP, and it had also a bad linearity for SH-ATP equilibrium data.

Adsorption thermodynamic parameters were observed from Table 6, the equilibrium data for adsorption were best represented by Langmuir model. Compared with the other models, the R^2 value were the highest. The calculated saturated adsorption capacities of Pb^{2+} and Cd^{2+} onto SH-ATP at the temperature of 288.15, 298.15, 308.15 and 318.15 K were 63.29, 65.79, 68.03, 78.13 mg/g and 19.38, 20.24, 21.32, 22.94 mg/g, respectively, which were basically the same as the saturated adsorption capacities in the experiment. Langmuir model had a favorable linearity for adsorption equilibrium data, and confirmed the monolayer coverage of Pb^{2+} and Cd^{2+} onto particles and the homogeneous distribution of active sites on SH-ATP, as Langmuir equation assumed that adsorbent surface was homogeneous. The Langmuir isotherm was found to be linear for SH-ATP over the entire concentration range studied.

The adsorption equilibrium constants (R_L) in the Langmuir model were calculated and plotted with the corresponding initial concentrations of Pb^{2+} and Cd^{2+}, the results were shown in Fig. 4. R_L (Huang et al., 2011) were all in the range of 0–1. And the larger initial concentrations of Pb^{2+} and Cd^{2+} were, the closer the R_L were to 0, it showed that the adsorption processes of Pb^{2+} and Cd^{2+} onto SH-ATP were inclined to occur. When the concentrations of Pb^{2+} and Cd^{2+} gradually increased, the adsorption processes presented more obvious irrelevance.

3.4. Calculation results of thermodynamic parameters

In order to understand the type of adsorption of SH-ATP to Pb^{2+} and Cd^{2+}, the thermodynamic parameters were calculated with the following equations (Zheng et al., 2018; Wang et al., 2019):

$$K_d = \frac{q_e}{c_e} \tag{3-1}$$

$$\Delta G = -RT\ln K_d \tag{3-2}$$

$$\ln K_d = \frac{\Delta S}{R} - \frac{\Delta H}{RT} \tag{3-3}$$

Where K_d is equilibrium adsorption distribution constant, ΔG is free energy change value of adsorption process (kJ/mol), ΔH

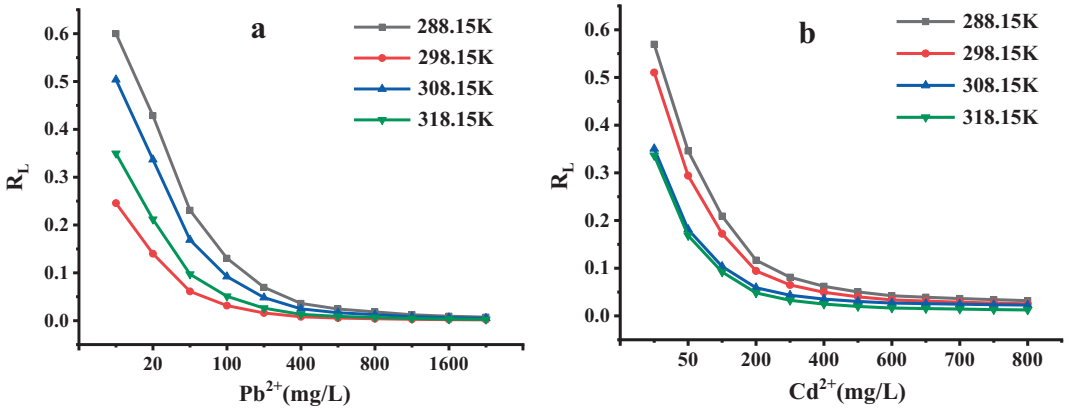

Fig. 4 Relationship between the R_L of Langmuir equation and the concentrations of Pb^{2+}(a) and Cd^{2+}(b).

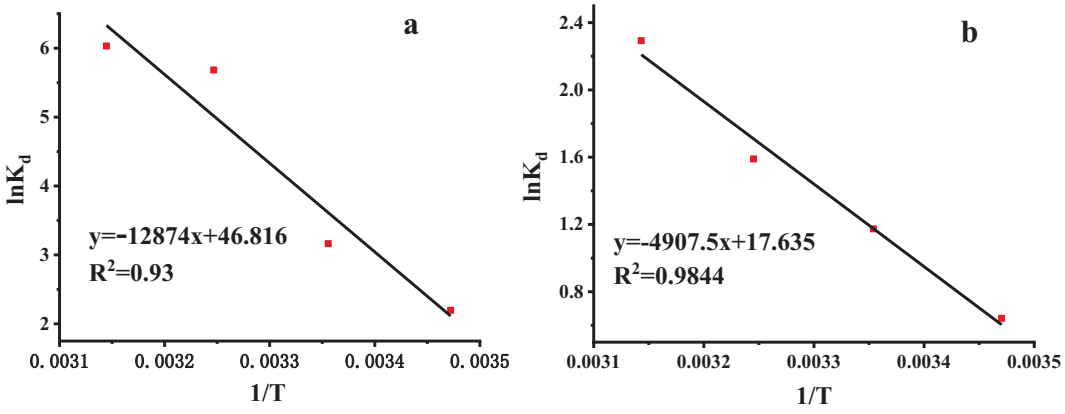

Fig. 5 Van't Hoff plot for Pb^{2+}(a) and Cd^{2+}(b)adsorption on SH-ATP.

is enthalpy change of adsorption process (kJ/mol), ΔS is adsorption entropy change (J/mol·K), c_e is equilibrium solution concentration (mg/L) when the adsorption capacity is q_e at T temperature, R is thermodynamic constant (8.314 J/(K·mol)), T is absolute temperature (K).

When c_e infinitely approached 0, the conclusion ($\ln q_e/c_e = -\ln K_d$) was obtained, and when the ordinate was the $\ln K_d$ and the abscissa was 1/T, the linear relationship were shown in Fig. 5. There was a good correlation between $\ln K_d$ and 1/T. The thermodynamic parameters ΔG, ΔH and ΔS of the adsorption processes were further calculated with equations (3-1), (3-2) and (3-3), as were shown in Table 7. The enthalpy change (ΔH^{2+}_{Pb} and ΔH^{2+}_{Cd}) were 107.03 kJ/mol and 40.801 kJ/mol, indicating that the adsorption reactions were endothermic, and the increase of temperature was beneficial to the reaction, which was consistent with the experimental results. The entropy change (ΔS^{2+}_{Pb} and ΔS^{2+}_{Cd}) were 389.22 J/mol·K and 146.62 J/mol·K, which was favourable to the spontaneous reaction. The free energy ($\Delta G < 0$) at different temperatures explained that the adsorption process was spontaneous, ΔG gradually increased with increasing temperature, the driving force of adsorption was also increased, it illustrated that the higher the temperature, the easier the reaction was.

Table 7 Thermodynamics data of Pb^{2+} and Cd^{2+} adsorption onto SH-ATP.

Metals ion	T (K)	ΔH (kJ/mol)	ΔG (kJ/mol)	ΔS (J/mol·K)
Pb^{2+}	288.15	107.034	−5.261	389.22
	298.15		−7.841	
	308.15		−14.551	
	318.15		−15.955	
Cd^{2+}	288.15	40.801	−1.538	146.62
	298.15		−2.909	
	308.15		−4.072	
	318.15		−6.063	

3.5. Adsorption mechanism

There may were many forces for SH-ATP to adsorb Pb^{2+} and Cd^{2+}, such as electrostatic attraction, ion exchange, surface and interlayer hydroxyl complexation, and grafted sulfhydryl complexation. When the concentrations of Pb^{2+} and Cd^{2+} were low, the adsorption processes were mainly physical adsorption. While the concentrations of Pb^{2+} and Cd^{2+} increased, the chemisorption adsorption became domination. Grafting sulfhydryl groups enhanced the complexing ability and the chemical adsorption capacity of SH-ATP to Pb^{2+} and Cd^{2+}. The process of adsorbing Pb^{2+} and Cd^{2+} onto SH-ATP was monolayer adsorption, the adsorbent surface was homogeneous, and the micropore distribution was relatively uniform. The adsorption process ($\Delta H > 0$, $\Delta G < 0$, $\Delta S > 0$) of Pb^{2+} and Cd^{2+} onto SH-ATP was endothermic and spontaneous, and the temperature rise was favorable for adsorption.

4. Conclusion

SH-ATP is a very good adsorbent. Its modification process is simple, the cost is low, and it has a well and applicable prospect. This work which study the adsorption amount, kinetics and thermodynamics of Pb^{2+} and Cd^{2+} onto SH-ATP, enable to lay the foundation for the practical application of SH-ATP.

(1) The saturated adsorption capacities of ATP and SH-ATP to Pb^{2+} and Cd^{2+} (25 °C) are 41.57 and 65.57 mg/g, 17.21 and 22.71 mg/g, respectively. Compared with the ATP, the saturated adsorption capacities of Pb^{2+} and Cd^{2+} have a significant enhancement, and increased by 57.74% and 31.96%, respectively.
(2) Adsorption kinetics indicates that the adsorption reactions of Pb^{2+} and Cd^{2+} may take place via surface exchange reactions until the surface functional sites are completely occupied, subsequently, the adsorption of Pb^{2+} and Cd^{2+} onto the SH-ATP will further interact such as ion-exchange and complexation.
(3) Adsorption thermodynamics shows that the surface of SH-ATP is homogeneous, the micropore distribution is also relatively uniform, and the adsorption of Pb^{2+} and Cd^{2+} are a monolayer adsorption.
(4) The adsorption enthalpy change ($\Delta H > 0$), entropy change ($\Delta S > 0$), adsorption reaction free energy ($\Delta G < 0$) illustrate that the adsorption processes are spontaneous, endothermic, and involve in entropic increase. So temperature rise is conducive to the reaction.

Acknowledgement

We gratefully acknowledge the financial support from the Science & Technology Department of Guizhou Province ([2019]2833 and [2019]1424). We also gratefully acknowledge the financial support from the Science & Technology Department of Sichuan Province (2019YFN0148).

References

Aliabadi, M., Irani, M., Ismaeili, J., Najafzadeh, S., Najafzadeh, S., 2014. Design and evaluation of chitosan/hydroxyapatite composite nanofiber membrane for the removal of heavy metal ions from aqueous solution. J. Taiwan Inst. Chem. 45, 518–526.

Arancibia-Miranda, N., Baltazar, S.E., Garcia, A., Munoz-Lira, D., Sepulveda, P., Rubio, M.A., 2016. Nanoscale zero valent supported by Zeolite and Montmorillonite: Template effect of the removal of lead ion from an aqueous solution. J. Hazard. Mater. 301, 371–380.

Barrios, M.S., González, L.V.F., Rodríguez, M.A.V., Pozas, J.M.M., 1995. Acid activation of a palygorskite with HCl: Development of physico-chemical, textural and surface properties. Appl. Clay Sci. 10, 247–258.

Bartczak, P., Norman, M., Klapiszewski, L., Karwanska, N., Kawalec, M., Baczynska, M., Wysokowski, M., Zdarta, J., Ciesielczyk, F., Jesionowski, T., 2018. Removal of nickel(II) and lead(II) ions from aqueous solution using peat as a low-cost adsorbent: A kinetic and equilibrium study. Arabian J. Chem. 11, 1209–1222.

Bhattacharyya, K.G., Sen Gupta, S., 2008. Adsorption of a few heavy metals on natural and modified kaolinite and montmorillonite: A review. Adv. Colloid Interface Sci. 140, 114–131.

Celis, R., Hermosín, M.C., Cornejo, J., 2000. Heavy metal adsorption by functionalized clays. Environ. Sci. Technol. 34, 4593–4599.

Eren, E., 2009. Removal of lead ions by Unye (Turkey) bentonite in iron and magnesium oxide-coated forms. J. Hazard. Mater. 165, 63–70.

Fan, Q.H., Shao, D.D., Hu, J., Wu, W.S., Wang, X.K., 2008. Comparison of Ni^{2+} sorption to bare and ACT-graft attapulgites: effect of pH, temperature and foreign ions. Surf. Sci. 602 (3), 778–785.

Freundlich, H.M.F., 1906. Over the adsorption in solution. J. Phys. Chem. 57, 385–470.

Gionis, V., Kacandes, G.H., Kastritis, I.D., Chryssikos, G.D., 2007. Combined Near-infrared and X-ray Diffraction Investigation of the Octahedral Sheet Composition of Palygorskite. Clays Clay Miner. 55, 543–553.

Huang, R.H., Wang, B., Yang, B.C., Zheng, D.S., Zhang, Z.Q., 2011. Equilibrium, kinetic and thermodynamic studies of adsorption of Cd(II) from aqueous solution onto HACC-bentonite. Desalination 280, 297–304.

Ijagbemi, C.O., Baek, M.H., Kim, D.S., 2010. Adsorptive performance of un-calcined sodium exchanged and acid modified montmorillonite for Ni^{2+} removal: Equilibrium, kinetics, thermodynamics and regeneration studies. J. Hazard. Mater. 174, 746–755.

Javadian, H., Ghorbani, F., Tayebi, H.A., Asl, S.H., 2015. Study of the adsorption of Cd (II) from aqueous solution using zeolite-based geopolymer, synthesized from coal fly ash; kinetic, isotherm and thermodynamic studies. Arabian J. Chem. 8, 837–849.

Karunanayake, A.G., Todd, O.A., Crowley, M., Ricchetti, L., Pittman, C.U., Anderson, R., Mohan, D., Mlsna, T., 2018. Lead and cadmium remediation using magnetized and nonmagnetized biochar from Douglas fir. Chem. Eng. J. 331, 480–491.

Kosak, A., Lobnik, A., Bauman, M., 2015. Adsorption of Mercury (II), Lead(II), Cadmium(II) and Zinc(II) from Aqueous Solutions Using Mercapto-Modified Silica Particles. Int. J. Appl. Ceram. Technol. 12, 461–472.

Krikorian, N., Martin, D.F., 2005. Extraction of Selected Heavy Metals Using Modified Clays. Environ. Lett. 40, 601–608.

Langmuir, I., 1918. The adsorption of gases on plane surfaces of glass, mica and platinum. J. Am. Chem. Soc. 40, 1361–1403.

Liang, X.F., Xu, Y.M., Sun, G.H., Wang, L., Sun, Y.B., Sun, Y., Qin, X., 2011. Preparation and characterization of mercapto functionalized sepiolite and their application for sorption of lead and cadmium. Chem. Eng. J. 174, 436–444.

Liang, X.F., Xu, Y.M., Tan, X., Wang, L., Sun, Y.B., Lin, D.S., Sun, Y., Qin, X., Wang, Q., 2013. Heavy metal adsorbents mercapto and amino functionalized palygorskite: Preparation and characterization. Colloids Surf. A 426, 98–105.

Ma, Y.L., Lv, L., Guo, Y.R., Fu, Y.J., Shao, Q., Wu, T.T., Guo, S.J., Sun, K., Guo, X.K., Wujcik, E.K., Guo, Z.H., 2017. Porous lignin based poly (acrylic acid)/organo-montmorillonite nanocomposites: Swelling behaviors and rapid removal of Pb (II) ions. Polymer 128, 12–23.

Mercier, L., Detellier, C., 1995. Preparation, characterization, and applications as heavy metals sorbents of covalently grafted thiol functionalities on the interlamellar surface of montmorillonite. Environ. Sci. Technol. 29, 1318–1323.

Mondal, M.K., 2009. Removal of Pb(II) ions from aqueous solution using activated tea waste: Adsorption on a fixed-bed column. J. Environ. Manage. 90, 3266–3271.

Revathi, M., Basha, C.A., Velan, M., 2016. Removal of copper (II) ions from synthetic electroplating rinse water using polyethyleneimine modified ion-exchange resin. Desalin. Water Treat. 57, 20350–20367.

Sarkar, B., Xi, Y.F., Megharaj, M., Naidu, R., 2011. Orange II adsorption on palygorskites modified with alkyl trimethylammonium and dialkyl dimethylammonium bromide-An isothermal and kinetic study. Appl. Clay Sci. 51, 370–374.

Tahir, S.S., Rauf, N., 2003. Thermodynamic studies of Ni(II) adsorption onto bentonite from aqueous solution. J. Chem. Thermodyn. 35 (12), 2003–2009.

Wang, J.Y., Li, Y.C., Lv, Z.M., Xie, Y., Shu, J.J., Alsaedi, A., Hayat, T., Chen, C.L., 2019. Exploration of the adsorption performance and mechanism of zeolitic imidazolate framework-8@graphene oxide for Pb(II) and 1-naphthylamine from aqueous solution. J. Colloid Interface Sci. 542, 410–420.

Wang, W.J., Chen, H., Wang, A.Q., 2007. Adsorption characteristics of Cd(II) from aqueous solution onto activated palygorskite. Sep. Purif. Technol. 55, 157–164.

Wang, Y.H., Wang, J.Q., Zhang, Y., Cao, D.Y., Li, R., 2012. Study on adsorption thermodynamics and kinetics of thermal-modified attapulgite clay. Journal of Textile Research. 33, 95–100.

Xiong, Q.X., Chen, W., Zhu, X.P., Hang, X., Zhao, Q.X., Liu, W.H., 2012. Kinetics and thermodynamics of adsorption of Pb^{2+} by mercapto-functionalized bentonite. Ion Exchange and Adsorption. 28, 432–441.

Yang, S.B., Chen, C.L., Chen, Y., Li, J.X., Wang, D.Q., Wang, X.K., Hu, W.P., 2015. Competitive Adsorption of Pb^{II}, Ni^{II}, and Sr^{II} Ions on Graphene Oxides: A Combined Experimental and Theoretical Study. Chempluschem. 80, 480–484.

Yariv, S., Borisover, M., Lapides, I., 2011. Few introducing comments on the thermal analysis of organoclays. J. Therm. Anal. Calorim. 105, 897–906.

Zeng, G.M., Wan, J., Huang, D.L., Hu, L., Huang, C., Cheng, M., Xue, W.J., Gong, X.M., Wang, R.Z., Jiang, D.N., 2017. Precipitation, adsorption and rhizosphere effect: The mechanisms for Phosphate-induced Pb immobilization in soils-A review. J. Hazard. Mater. 339, 354–367.

Zhang, X., Lin, S., Lu, X.Q., Chen, Z.L., 2010. Removal of Pb(II) from water using synthesized kaolin supported nanoscale zero-valent iron. Chem. Eng. J. 163, 243–248.

Zhang, Y., Wang, W.B., Zhang, J.P., Liu, P., Wang, A.Q., 2015. A comparative study about adsorption of natural palygorskite for methylene blue. Chem. Eng. J. 262, 390–398.

Zheng, H.L., Gao, Y., Zhu, K.R., Wang, Q., Wakeel, M., Wahid, A., Alharbi, N.S., Chen, C.L., 2018. Investigation of the adsorption mechanisms of Pb(II) and 1-naphthol by b-cyclodextrin modified graphene oxide nanosheets from aqueous solution. J. Colloid Interface Sci. 530, 154–162.

Zhu, X.P., Liu, H., Tang, J., Liu, W.H., Feng, C., 2013a. Mechanism study of cadmium(Ⅱ) adsorption on thiol-modified montmorillonite. Rock Min. Anal. 32, 613–620.

Zhu, Y.K., Chen, T.H., Liu, H.B., Xu, B., Xie, J.J., 2016. Kinetics and thermodynamics of Eu(III) and U(VI) adsorption onto palygorskite. J. Mol. Liq. 219, 272–278.

Zhu, Z., Gao, C., Wu, Y.L., Sun, L.F., Huang, X.L., Ran, W., Shen, Q.R., 2013b. Removal of heavy metals from aqueous solution by lipopeptides and lipopeptides modified Na-montmorillonite. Bioresour. Technol. 147, 378–386.